HAPTIC INTERACTION WITHIN A PLANAR ENVIRONMENT

S. P. DiMaio, S. E. Salcudean and M. R. Sirouspour
Department of Electrical and Computer Engineering
University of British Columbia
Vancouver, BC, V6T 1Z4, Canada
tims@ece.ubc.ca

ABSTRACT

A haptic simulation environment to simulate planar three-degree-of-freedom motion has been developed by the authors. The system consists of a novel parallel manipulandum and associated control, collision detection and dynamic simulation software running on a QNX PC. This paper describes haptic interface control and outlines the control systems that have been designed for the haptic rendering of virtual environments. Virtual environment design and implementation are also discussed. Using the haptic simulation environment that has been developed, a four-channel teleoperation architecture is shown to be an effective means to display a variety of simulated environments and is compared with a popular impedance-based approach.

INTRODUCTION

Several haptic interaction systems have been developed in the past. Most of these have addressed point interaction (see for example Zilles and Salisbury, 1995), while only a few have addressed rigid-body interaction (see Chang and Colgate, 1997). Some of the most complete rigid-body simulations, to date, have been reported in (Cohen and Chen, 1999) and in (Berkelman *et al*, 1999), which describes the 6-DOF haptic interaction of a magnetically levitated haptic device with the dynamic simulator developed by (Baraff, 1995). Such systems present several challenges for the design of haptic interface mechanisms, the simulation of virtual environments as well as for haptic control.

The haptic simulation environment described in this paper comprises a planar 3-DOF haptic device with parallel and redundant actuation; an observer that estimates hand forces and velocities applied to the haptic interface, without direct measurement; virtual slave and environment models; a controller that coordinates both force and position information between the haptic device and the virtual environment; and a graphical display, all depicted in Figure 1. With respect to other haptic interaction systems,

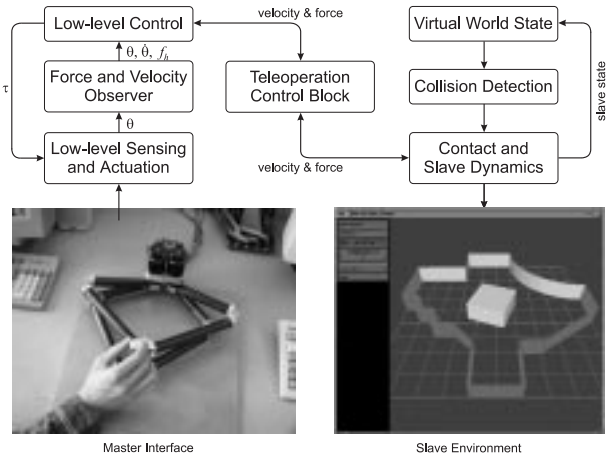

Figure 1. The virtual environment system architecture.

this approach allows a reasonable motion range (the motion range available in (Berkelman *et al*, 1999) is small), significant forces and torques (the torque level available in (Cohen and Chen, 1999) is small), and decouples interactive virtual environment design from haptic controller design.

The paper begins with a description of the haptic simulation system architecture and is followed by an outline of the haptic device design, its dynamics, actuation and sensing. Interface control, virtual environment simulation and their implementation within a teleoperation framework are detailed and evaluated experimentally. Finally, concluding remarks and scope for future work are presented.

HAPTIC SIMULATION ARCHITECTURE

A typical haptic display system comprises three majour components, namely: (i) the haptic interface that measures positions and forces applied by the user's hand, and that applies feedback forces on the hand; (ii) a virtual environment that includes both tool and environment dynamic models; and (iii) a control system that coordinates the haptic interface and virtual environment simulation. The issue of haptically rendering interactive virtual environments is essentially a teleoperation problem in which the haptic interface and the virtual tool are almost always both kinematically and dynamically dissimilar, resulting in some difficulty in realizing transparent interaction between the user and the synthetic environment (Salcudean, 1997).

For haptic displays, direct coupled *impedance* and *admittance* simulations have been proposed (Adams *et al*, 1998; Yoshikawa and Ueda, 1996; Nahvi *et al*, 1998). *Virtual couplings* have also been used (see Colgate *et al*, 1995). Impedance display, the more widespread of these, passes sensed hand positions to the dynamic simulator, while forces are returned from the environment. This is essentially a two-channel approach. The transmission of positions and forces in both directions between master and slave has been found to be important for achieving high performance in teleoperation systems (Lawrence, 1993; Salcudean, 1997).

We employ a novel multi-channel architecture for haptic simulation, as well as the use of an explicitly modelled *virtual slave* that is designed independently of the haptic control system. A four-channel coupling between the haptic interface and dynamic simulation allows the interface to behave either as a force sensor, or as a position sensor depending upon the impedance of the virtual environment, and is therefore a hybrid of the two traditionally adopted approaches (Salcudean, 1997; Sirouspour, 2000). This strategy is evaluated within a haptic simulation system described in subsequent sections.

THE PLANAR PANTOGRAPH HAPTIC INTERFACE

The haptic interface has three degrees of freedom allowing for translation in a plane Π and unlimited rotation about an axis orthogonal to Π. This is achieved by using a dual pantograph arrangement, as shown in Figure 2. Each pantograph is driven by two DC motors located at the base joints, while their endpoints are coupled by means of a linkage, to which the interface handle is connected. This linkage forms a crank that allows for unlimited rotation of the handle.

Mechanism Dynamics

An accurate model of haptic interface dynamics is desirable for control purposes and begins with the derivation of

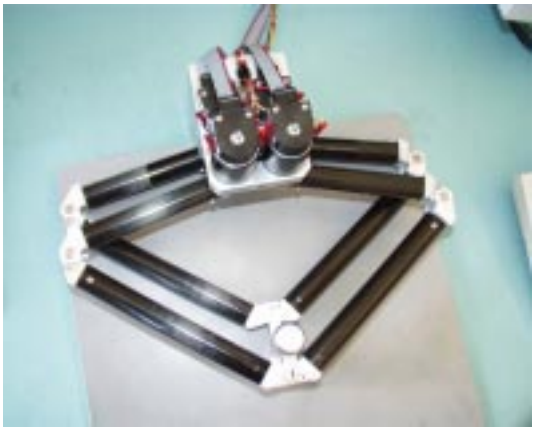

Figure 2. The three-degree-of-freedom planar pantograph interface.

the equations of motion using the Euler-Lagrange approach (Spong and Vidyasagar, 1989). The equations of motion for a single pantograph in actuated joint variables, $\theta = [\theta_1\ \theta_2]^T$, are expressed in terms of the parameters shown in Figure 3:

$$D_p(\theta)\ddot{\theta} + C_p(\theta,\dot{\theta})\dot{\theta} = \tau_p - J_e^T F_e = \tau + \tau_{env}\ , \qquad (1)$$

where τ_p is a vector of the applied actuator torques, J_e is the manipulator Jacobian and F_e is the hand force applied to the end-effector. Mass and Christoffel matrices D_p and C_p are also present. The equations of motion describing the

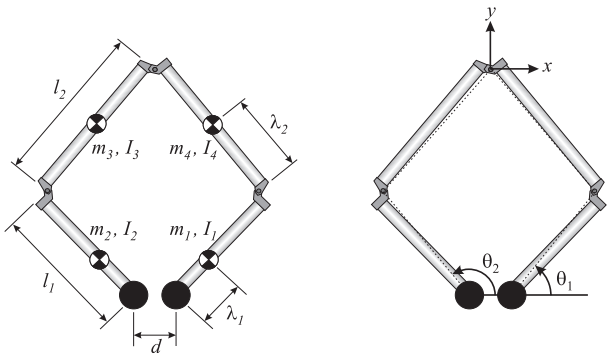

Figure 3. Pantograph configuration and parameters.

workspace dynamics of two coupled pantographs take the following standard form (see Sirouspour, 2000 for details):

$$M_c\ddot{X}_c + C_c\dot{X}_c = F_h + J_c^T\tau = F_h + u\ , \qquad (2)$$

where X_c is a vector of interface handle coordinates $[x_c\ y_c\ \alpha]$, F_h is the hand force acting on the interface handle and τ is a vector of actuator torques. The internal force acting longitudinally along the linkage bar does not affect the system dynamics since the actuator torques which constitute this force lie in the null space of J_c^T. Note that as the pantographs are oriented horizontally, there are no gravity terms. Friction is insignificant and can be neglected.

Actuation and Sensing

Four 90W DC motors provide actuation at the active pantograph joints and are considered, for the purposes of control, to be torque sources. Each of the four joint angles is measured by a digital optical encoder with a resolution of 0.09 degrees. Velocities, accelerations and forces are not directly measurable and are computed purely from joint angle measurements and applied motor torques by using a system state observer (Hacksel and Salcudean, 1994). Given an accurate dynamic model, as well as measured joint angles and applied actuator forces, the system states (angular joint velocity) and unknown external disturbances (hand force applied to the interface end-effector) can be observed and computed, as indicated in Figure 4. This approach has

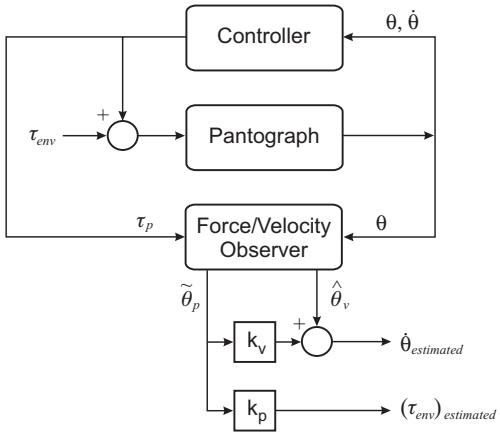

Figure 4. Force observation using only applied actuator torques and measured joint angles.

been demonstrated for a single free body (Hacksel and Salcudean, 1994), but is shown here to be applicable to a parallel mechanism (a single pantograph mechanism), by using a simplified Nicosia Observer (Nicosia and Tomei, 1990):

$$\begin{aligned}\dot{\hat{\theta}}_p &= \hat{\theta}_v + k_v\tilde{\theta}_p \\ \dot{\hat{\theta}}_v &= D_p(\theta)^{-1}(-C_p(\theta,\hat{\dot{\theta}}_p)\hat{\dot{\theta}}_p + k_p\tilde{\theta}_p + \tau_p)\ , \end{aligned} \qquad (3)$$

where $\hat{\theta}_p$ and $\hat{\theta}_v$ are angular position and velocity states, $\tilde{\theta}_p$ is the position state estimation error $(\theta - \hat{\theta}_p)$, k_v and k_p are state feedback gains. The matrices D_p and C_p are defined in (1). By combining (3) with pantograph equations of motion (1), the error dynamics become:

$$\begin{aligned} D_p(\theta)\ddot{\tilde{\theta}}_p + (C_p(\theta,\dot{\theta}) + C_p(\theta,\hat{\dot{\theta}}_p) + k_v D_p(\theta))\dot{\tilde{\theta}}_p + \ \ldots \\ + k_p\tilde{\theta}_p = J_e^T F_e = \tau_{env} \end{aligned}$$

At steady-state, the effective joint torques due to applied hand forces, τ_{env}, are related to joint angle estimation errors by a simple stiffness relationship, $\tau_{env} = k_p\tilde{\theta}_p$. The observer also provides an estimate of joint velocities, in the presence of hand forces:

$$\dot{\theta}_{estimated} = \dot{\hat{\theta}}_p = \hat{\theta}_v + k_v\tilde{\theta}_p\ .$$

The selection of observer state feedback gains k_p and k_v is made such that the error $\tilde{x}$, and consequently the hand force estimate, converge as quickly as possible. Their magnitudes are bounded by the presence of joint angle measurement noise. Figure 5 shows a comparison of hand forces predicted off-line by an inverse dynamic model, with those estimated by the on-line force observer. The observer clearly tracks

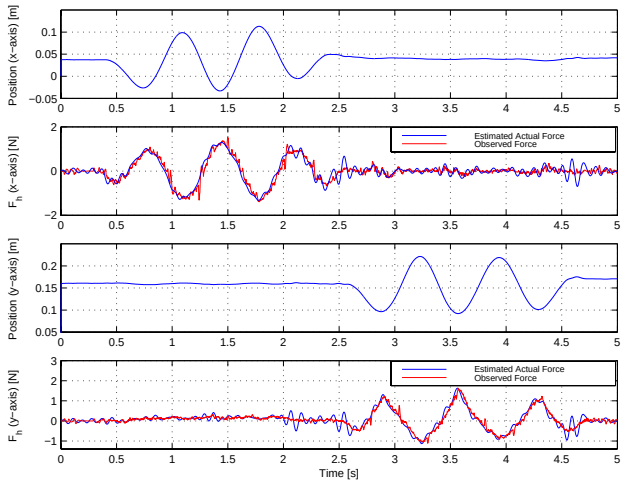

Figure 5. Force observer performance.

the applied hand force closely. A relatively low observer bandwidth, limited by the coarse joint angle resolution, results in some degradation of the force and velocity observations at higher frequencies (above 10Hz). Force estimates for each pantograph mechanism are combined in order to determine the hand force applied to the interface handle.

VIRTUAL ENVIRONMENT SIMULATION

Both rigid and non-rigid environment models have been implemented for haptic display. For virtual rigid constraints, we use a passive 3-DOF contact model that is based upon a spring-damper model with predictor-corrector force discretisation (see Ellis *et al*, 1996). A reset-integrator, dry friction model, devised by (Haessig and Friedland, 1991), is also included. The experimental evaluation of these, and other rigid contact models, is given in (Constantinescu *et al*, 2000), along with the implementation of the fast collision detection algorithm that has been used.

Deformable materials are simulated for non-rigid contact modelling using a 2-D Finite Element discretisation method. For example, a rectangular block is discretised as

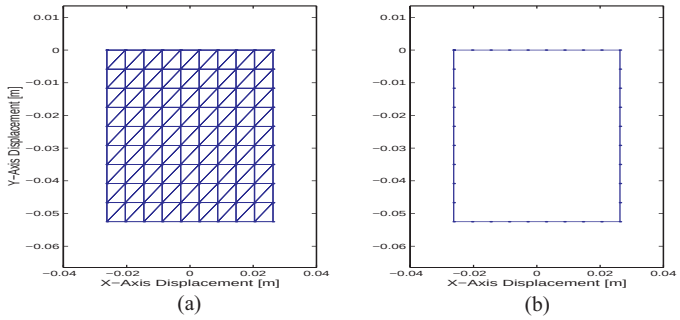

Figure 6. Finite Element representation of the environment: (a) finite elements and mesh nodes; and (b) boundary nodes.

shown in Figure 6(a). For linear elastic materials, the total strain energy E_{strain} over a solid body Ω,

$$E_{strain} = \frac{1}{2}\int_{\Omega} \epsilon^T(x)\sigma(x)dx \ , \qquad (4)$$

is minimum at static equilibrium, where ϵ and σ are stress and strain vectors respectively. Each element e reaches its static equilibrium state when the first variation of the energy functional δE^e vanishes. After discretising (4) using linear shape functions (see Curvelier, *et al* 1986), this is expressed as:

$$\delta E^e = \int_{\Omega^e} A^e \underline{u}^e dx - \underline{f}^e = 0 \ , \qquad (5)$$

where the A^e matrix characterises the elastic behaviour of element Ω^e (see Curvelier, 1986) and $\underline{u}^e$ and $\underline{f}^e$ are displacement and force vectors for those mesh nodes that constitute element e. Over the entire set of nodes on body Ω, this leads to a set of $2n$ linear equations $K_{(2n\times 2n)}\underline{u} = \underline{f}$. Since we are interested only in interactions with boundary nodes, matrix K can be condensed, resulting in a reduced set of $2s$ linear equations, $K'_{(2s\times 2s)}\underline{u}' = \underline{f}'$, where s is the number of boundary nodes. Reaction forces due to forced displacement at contact nodes, as well as the displacements of unconstrained boundary nodes, are easily computed by solving this set of equations. Fundamental solutions, arising from single contact point displacements are precomputed to permit real-time simulation (similar to Cotin *et al*, 1996).

CONTROL SYSTEM ARCHITECTURE

The twin pantograph interface provides the operator with a means of interacting with the virtual environment. The operator should feel the dynamics of a virtual object/tool in free motion and environment forces during contact phases, while the operator hand force and motion are conveyed to the virtual object. A dual stage control strategy is adopted and consists of interface control and teleoperation control subsystems. This approach is presented in detail in (Sirouspour, 2000) and is summarised here.

Interface Control

An impedance control law has been derived in order to shape the device dynamics to match those of the virtual tool. This greatly simplifies teleoperation controller development. If the apparent mass of the device is to be changed, then a measure of the hand force, or equivalently the device acceleration, is required and is provided by the force/velocity observer. In practice, the interface controller was able to achieve a perceived mass ranging between one half and ten times the physical mass of the device.

Since there is redundancy in the actuation system, the set of motor torques τ required for any given end-effector force and torque u, is not unique. Consequently, motor torques are selected in order to minimise the internal force applied longitudinally on the connecting bar.

Teleoperation Control

Though our problem is primarily a haptic simulation, a tele-operation control strategy is adopted to coordinate the hand controller with the virtual object. In this approach, the master is the haptic device interacting with a human operator, while the slave is replaced by the dynamic simulator software. We use the general teleoperation architecture proposed in (Lawrence, 1993). It utilizes four types of data transmission between master and slave, sending forces and positions in both directions, as shown in Figure 7. In a

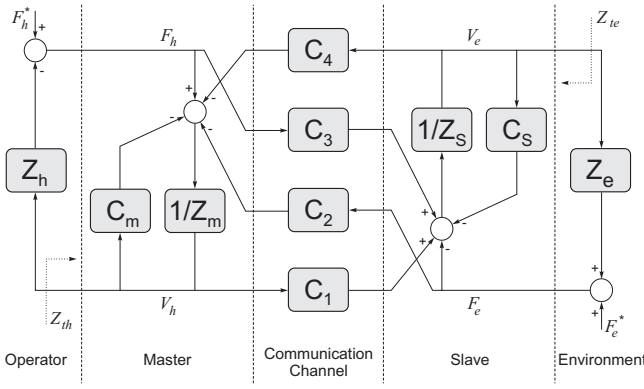

Figure 7. Four-channel architecture.

haptic simulation, the slave and environment are virtual, so that the dynamic simulator replaces Z_s and Z_e. The advantage of employing existing controller design methods that are based upon this architecture is that the controller can be designed independently of the virtual environment models, as long as these can be presumed passive (Lawrence, 1993).

EXPERIMENTAL RESULTS

In an implementation of the haptic display, the user manipulates a virtual rectangular block within a simulated

environment that contains both rigid and non-rigid constraints, rendered by physically-based contact models. Haptic interface control, virtual environment simulation and teleoperation control are computed in real-time at a 500Hz sampling rate by a PC running QNX4, with I/O performed by a Quanser Multi-Q-3^{TM} card.

Several two- and four-channel teleoperation control algorithms were implemented for the haptic display of both the rigid and deformable planar environments described previously, using the planar pantograph interface. While this section presents a comparison of two control algorithms, the reader is referred to (Sirouspour *et al*, 2000) for further details and experimental results.

The impedance controller was designed to match the dynamics of the twin pantograph device with those of a 4.2cm-by-2.1cm virtual rectangular block having a mass of 2kg and moment of inertia of $0.0016\mathrm{kg}\,m^2$. The resulting equations of motion are linear and decoupled in each coordinate; therefore, the teleoperation controllers were designed separately for each degree of freedom. The performance of a two channel position-force architecture and a transparent four channel architecture, with adaptive damping, are compared. Each architecture is evaluated for the display of two contact tasks. The first is a rigid peg-in-hole type insertion and the second is the prodding of a "sticky" elastic material, as illustrated in Figures 8 and 9.

(a) Two-channel teleoperation

In the first experiment, a two channel position-force architecture was used for haptic simulation. This is similar to an impedance simulation approach. The y-axis and α-axis (rotation) controller parameters were chosen as ($C_1^{(y)} = C_s^{(y)} = 40 + \frac{400}{s}$, $C_m^{(y)} = C_4^{(y)} = 0$, $C_2^{(y)} = 1$, $C_3^{(y)} = 0$) and ($C_1^{(\alpha)} = C_s^{(\alpha)} = 0.004 + \frac{0.5}{s}$, $C_m^{(\alpha)} = C_4^{(\alpha)} = 0$, $C_2^{(\alpha)} = 1$, $C_3^{(\alpha)} = 0$) respectively (making use of Laplace notation and SI units). C_1 and C_s form a coordinating force controller for virtual slave position tracking, while the environment force is fed back to the master through C_2. The results are presented in Figures 8(a), 8(b), 9(a) and 9(b).

(b) Four-channel with adaptive damping

This experiment was conducted using ($C_m^{(y)} = C_s^{(y)} = 20 + \frac{100}{s}$, $C_1^{(y)} = C_s^{(y)}$, $C_4^{(y)} = -C_m^{(y)}$, $C_2^{(y)} = C_3^{(y)} = 1$) and ($C_m^{(\alpha)} = C_s^{(\alpha)} = 0.04 + \frac{0.5}{s}$, $C_1^{(\alpha)} = C_s^{(\alpha)}$, $C_4^{(\alpha)} = -C_m^{(\alpha)}$, $C_2^{(\alpha)} = C_3^{(\alpha)} = 1$). Environment and hand forces are fed forward to the master and slave with unity gains, while coordinating force control is introduced through the position channels (C_1 and C_4) and local controllers (C_m and C_s). To remove the force chattering, an adaptive damping term was added to both the master and slave controllers (Salcudean *et al*, 1995):

$$C_m^{(y)} = 20 + \frac{100}{s} + B_{madp}^{(y)}\ ,\ B_{madp}^{(y)} = K_{mb}^{(y)}|f_e^{(y)}| + B_{min}\ ,$$
$$C_s^{(y)} = 20 + \frac{100}{s} + B_{sadp}^{(y)}\ ,\ B_{sadp}^{(y)} = K_{sb}^{(y)}|f_e^{(y)}| + B_{min}\,,$$

with $K_{mb}^{(y)} = 5\mathrm{s/m}$, $K_{mb}^{(\alpha)} = 1\mathrm{s/m}$, $K_{sb}^{(y)} = 2\mathrm{s/m}$, $K_{sb}^{(\alpha)} = 1\mathrm{s/m}$, $B_{min} = 0\mathrm{kg/s}$, and f_e the environment force.

Figures 8(c), 8(d), 9(c) and 9(d) show the position and force tracking during during interaction with both virtual environments.

We observe that while force tracking is good, the two-channel algorithm loses position tracking during environment contact. This is a significant drawback of the approach. Improved position tracking is obtained by including two additional channels within the four-channel architecture. It is important to note that the position tracking performance of the two-channel position-force architecture is dependent primarily upon coordinating force controllers C_1 and C_s. For accurate tracking, it is necessary to use high position and velocity gains. In theory, perfect position tracking is possible, given an infinite position gain, while in practice, these gains are bounded by the effects of measurement noise. This is evident in Figures 8(a) and 9(a), where the y-axis position and velocity gains have been limited in order to maintain a force signal-to-noise ratio similar to that attained by the four channel algorithm. These gains can be increased to significantly improve position tracking, but with a noticeable increase in response noise. Lower position and velocity gains are tolerated under four-channel control, due to the presence of the additional force and velocity channels.

CONCLUSIONS AND FUTURE WORK

This paper has outlined the design and evaluation of a novel haptic display system. In an experimental virtual environment consisting of a new 3-DOF planar haptic interface, a novel force observer and physically-based slave and environment models, a teleoperation control framework is shown to be effective for haptic rendering. The advantage of this approach is that it provides a clear and general methodology for interactive virtual environment design. The explicit modelling of a virtual slave means that complex, multi-body and perhaps time varying slave behaviour is easily incorporated, independent of the haptic interface or its associated control system. This is in contrast to the traditional approach in which slave dynamics are often implied within the haptic interface control system itself.

Based on the experimental results, a four-channel teleoperation framework, augmented with adaptive damping, performs very well both in free motion and during contact

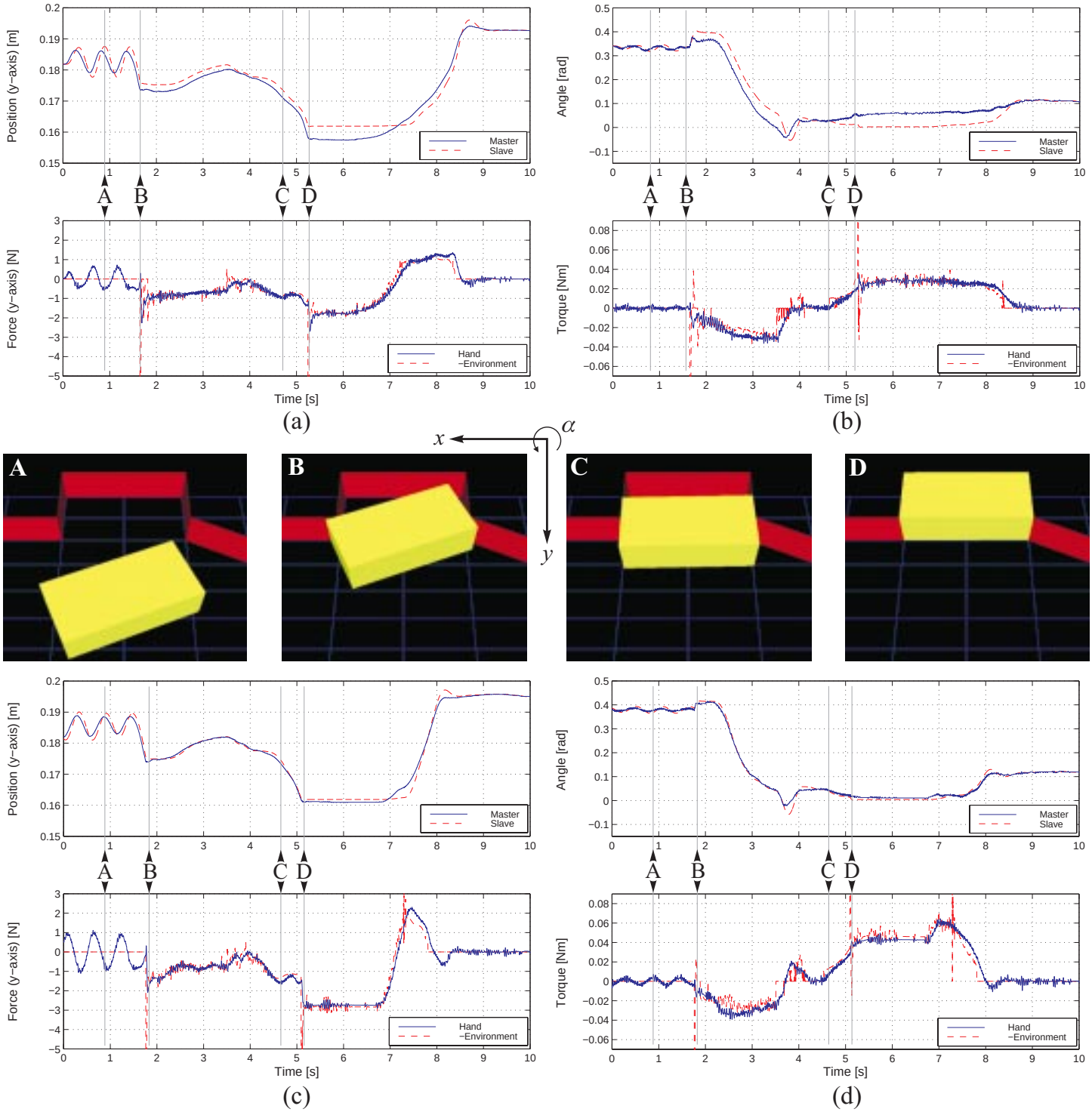

Figure 8. Haptic display of an insertion task within the rigid virtual environment, with two-channel position and force tracking in (a) y-axis and (b) α-axis; four-channel position and force tracking in (c) y-axis and (d) α-axis. Significant events occur at A, B, C and D. The slave is in free motion at A, collides with hole entrance at B, is sliding into hole at C and collides with back wall at D. Finally, the virtual slave is withdrawn from the hole.

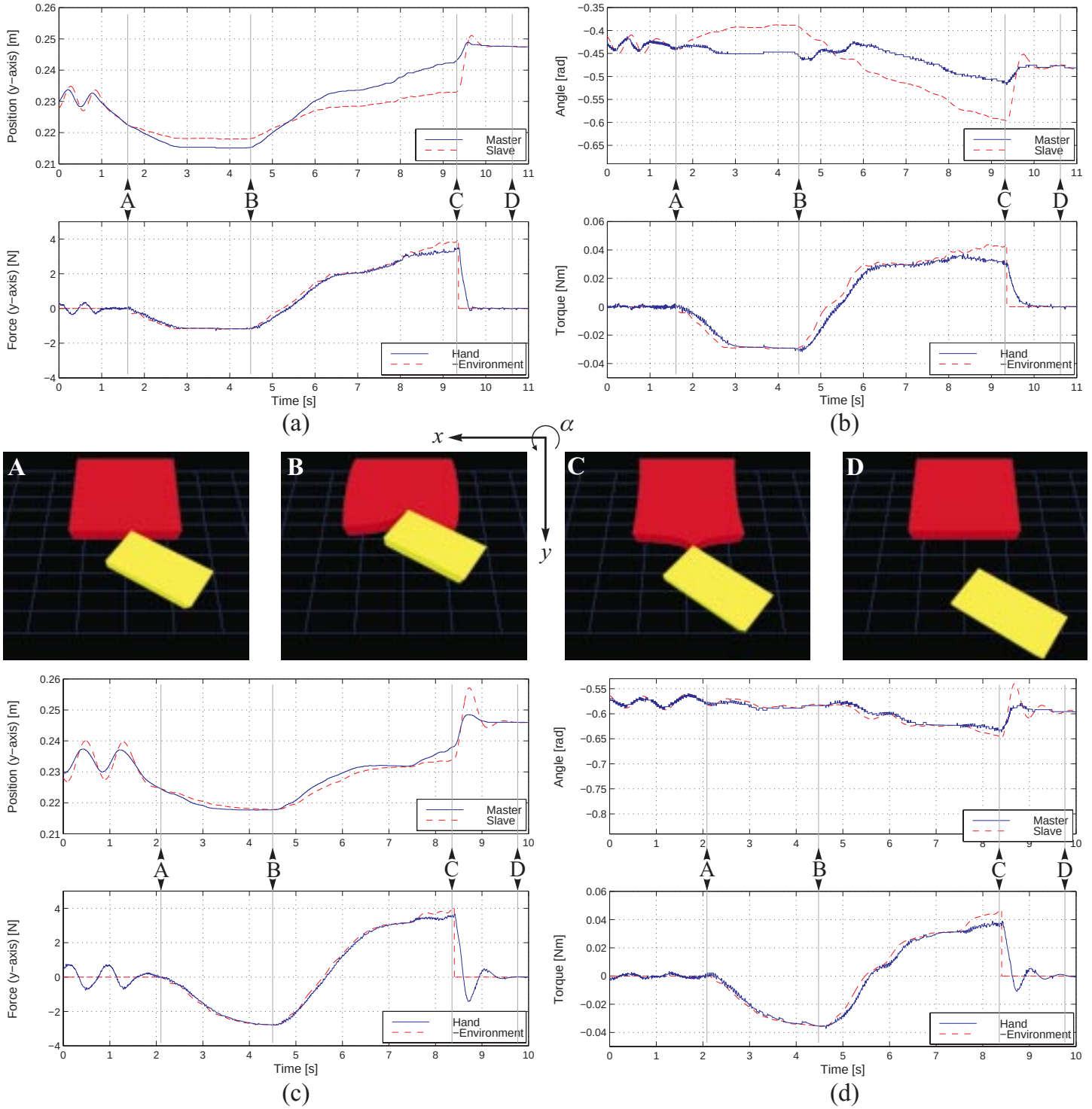

Figure 9. Haptic display of interaction with a "sticky" deformable virtual environment, with two-channel position and force tracking in (a) y-axis and (b) α-axis; four-channel position and force tracking in (c) y-axis and (d) α-axis. Significant events occur at A, B, C and D. The slave is in free motion prior to A, makes contact with the environment at A, is pushed into a deforming environment at B, is pulled away from the "sticky" environment and breaks contact with the environment at C. At point D, the slave is in free motion.

phases. Good performance is achieved using two quite different contact environment models, with the control system remaining unchanged between models. The two-channel control architecture exhibits good force tracking, but is unable to attain comparable position tracking during contact. The additional feedforward hand force, in particular, allows the four-channel controller to apply environment position constraints without a position penalty, either in the environment, or between master and slave.

Future work includes improvements and further evaluation of force observer accuracy and bandwidth, as well as the incorporation of more complex slave dynamics. Further optimization of the trade-off between system transparency and stability is also required of the controller design.

ACKNOWLEDGMENTS

The authors would like to thank Leo Stocco and Simon Bachmann for their assistance. This work was supported by the Canadian IRIS/PRECARN Network of Centers of Excellence.

REFERENCES

Zilles, C.B. and Salisbury, J.K., "A Constraint-based God Object Method for Haptic Display." In *IEEE Int. Conf. Intel. Rob. and Syst.*, Vol. 3, pages 146-151, Piscataway, NJ, 1995.

Chang, B. and Colgate, J.E., Real-Time Impulse-Based "Simulation of Rigid Body Systems for Haptic Display." In *Proc. ASME, Dyn. Sys. and Ctrl Div.*, pages 1-8, Houston, 1997.

Cohen, A. and Chen, E., "Six Degree-of-Freedom Haptic System as a Desktop Virtual Prototyping Interface." In *Proc. ASME, Dyn. Sys. and Ctrl. Div.*, Vol. 67, pages 401-402, 1999.

Berkelman, P.J., Hollis, R.L. and Baraff, D., "Interaction with a Realtime Dynamic Environment Simulation using a Magnetic Levitation Haptic Interface Device." In *Proc. IEEE Intl. Conf. Robotics and Automation*, pages 3261-3266, Detroit, May 1999.

Baraff, D., "Interactive Simulation of Solid Rigid Bodies." *IEEE Computer Graphics and Applications*, Vol. 15, pages 63-75, 1995.

Salcudean, Septimiu E., "Control for Teleoperation and Haptic Interfaces." In *Lecture Notes in Control and Information Sciences 230 – Control Problems in Robotics and Automation*, Springer-Verlag, pages 51-65, 1997.

Adams, Richard J., Moreyra, Manuel R. and Hannaford, Blake, "Stability and Performance of Haptic Displays: Theory and Experiments." In *Proceedings of the ASME, Dynamic Systems and Control Division*, Anaheim, CA, pages 227-234, 1998.

Yoshikawa, T. and Ueda, H., "Construction of Virtual World Using Dynamics Modules and Interaction Modules." In *Proc. IEEE Intl. Conf. on Rob. and Auto.*, pages 2358-2364, 1996.

Nahvi, A., Nelson, D.D., Hollerbach, J.M. and Johnson, D.E., "Haptic Manipulation of Virtual Mechanisms from Mechanical CAD Designs." In *Proc. IEEE Intl Conf. on Robotics and Automation*, Leuven, Belgium, pages 375-380, May 1998.

Colgate, J.E., Stanley, M.C. and Brown, J.M., "Issues in the Haptic Display of Tool Use." In *Proc. IEEE/RSJ Intl Conf. on Intel. Robots and Sys.*, Pittsburgh, pages 140-145, 1995.

Lawrence, D.A., "Stability and Transparency in Bilateral Teleoperation." In *IEEE Transactions on Robotics and Automation*, Vol. 9, No. 5, pages 624-637, 1993.

Spong, Mark W. and Vidyasagar, M., "Robot Dynamics and Control." Published by *Wiley*, 1989.

Sirouspour, M.R., DiMaio, S.P., Salcudean, S.E., Abolmaesumi, P. and Jones, C., "Haptic Interface Control - Design Issues and Experiments with a Planar Device," *IEEE Intl Conf. on Robotics and Automation*, San Francisco, CA, April 2000.

Hacksel, P.J. and Salcudean, S.E., "Estimation of Environment Forces and Rigid-Body Velocities using Observers." In *Proceedings of the IEEE International Conference on Robotics and Automation*, San Diego, CA, pages 931-936, May 1994.

Nicosia, S. and Tomei, P., "Robot control by using only joint position measurements." In *IEEE Transactions on Automatic Control*, pages 1058-1061, September, 1990.

Ellis, R.E., Sarkar, N. and Jenkins, M.A., "Numerical Methods for the Haptic Presentation of Contact: Theory, Simulations, and Experiments." In *Proc. ASME, Dynamic Sys. and Control Div.*, volume DSC-58, pages 413-420, New York, NY, 1996.

Haessig, D.A. Jr. and Friedland, B., "On the Modelling and Simulation of Friction." In *Journal Dyn. Syst. Meas. Contr.*, DSC-113, pages 354-362, 1991.

Constantinescu, D., Chau, I., DiMaio, S.P., Filipozzi, L., Salcudean, S.E. and Ghassemi, F., "Haptic Rendering of Planar Rigid-Body Motion using a Redundant Parallel Mechanism." *IEEE Intl Conf. on Rob. and Autom.*, April 2000.

Salcudean, S.E., Wong, M. and Hollis, R.L., "Design and Control of a Force-Reflecting Teleoperation System with Magnetically Levitated Master and Wrist." In *IEEE Transactions on Robotics and Automation*, Vol. 11, December 1995.

Curvelier, C., Segal, A. and van Steenhoven A.A, "Finite Element Methods and Navier-Stokes Equations." D. Reidel Publishing Company, 1986.

Cotin, S., Delingette, H., Bro-Nielsen M., Ayache N., Clement, J.M., Tassetti V. and Marescaux, J., "Geometric and Physical Representations for a Simulator of Hepatic Surgery". In *Medicine Meets Virtual Reality IV, Interactive Technology and the New Paradigm for Healthcare*, pages 139-151. January 1996.